

**Multibody analysis of a ride simulator for  
a two-wheeled vehicle  
(European MORIS project)**

**Ricardo Testi - Technical Innovation -Engine Division**

**Piaggio & C. spa- ITALY**

## CONTENTS

1. OBJECT OF THE ANALYSIS .....	3
2. THE PHYSICAL SYSTEM AND THE MULTIBODY MODEL.....	3
3. THE LOADS .....	4
4. THE STRUCTURE OF THE MODEL.....	8
5. ONE OF THE ANALYSED CASES: LANE CHANGE MANOEUVRE .....	9
6. CONCLUSIONS .....	16

## PICTURES

Picture 1. The physical system. ....	3
Picture 2. The multibody model. ....	4
Picture 3. The loads. ....	5
Picture 4. xy view of the actuators. ....	6
Picture 5. xz view of the actuators. ....	7
Picture 6. yz view of the actuators.....	8
Picture 7. Control matrixes structure.....	8
Picture 8. Flow chart describing how the model works. ....	8
Picture 9. Lane change manoeuvre. Target acceleration components time histories. ....	9
Picture 10. Lane change manoeuvre. Power of the actuators #1, 2 and 3. ....	11
Picture 11. Lane change manoeuvre. Power of the actuators # 4, 5 and 6. ....	12
Picture 12. Lane change manoeuvre. Velocity of the pistons the actuators #1, 2 and 3, relative to the cylinders.....	13
Picture 13. Lane change manoeuvre. Velocity of the pistons the actuators #4, 5 and 6, relative to the cylinders.....	14
Picture 14. Lane change manoeuvre. Reference point displacement. ....	15
Picture 15. Lane change manoeuvre. Reference point rotations. ....	16

## 1. OBJECT OF THE ANALYSIS

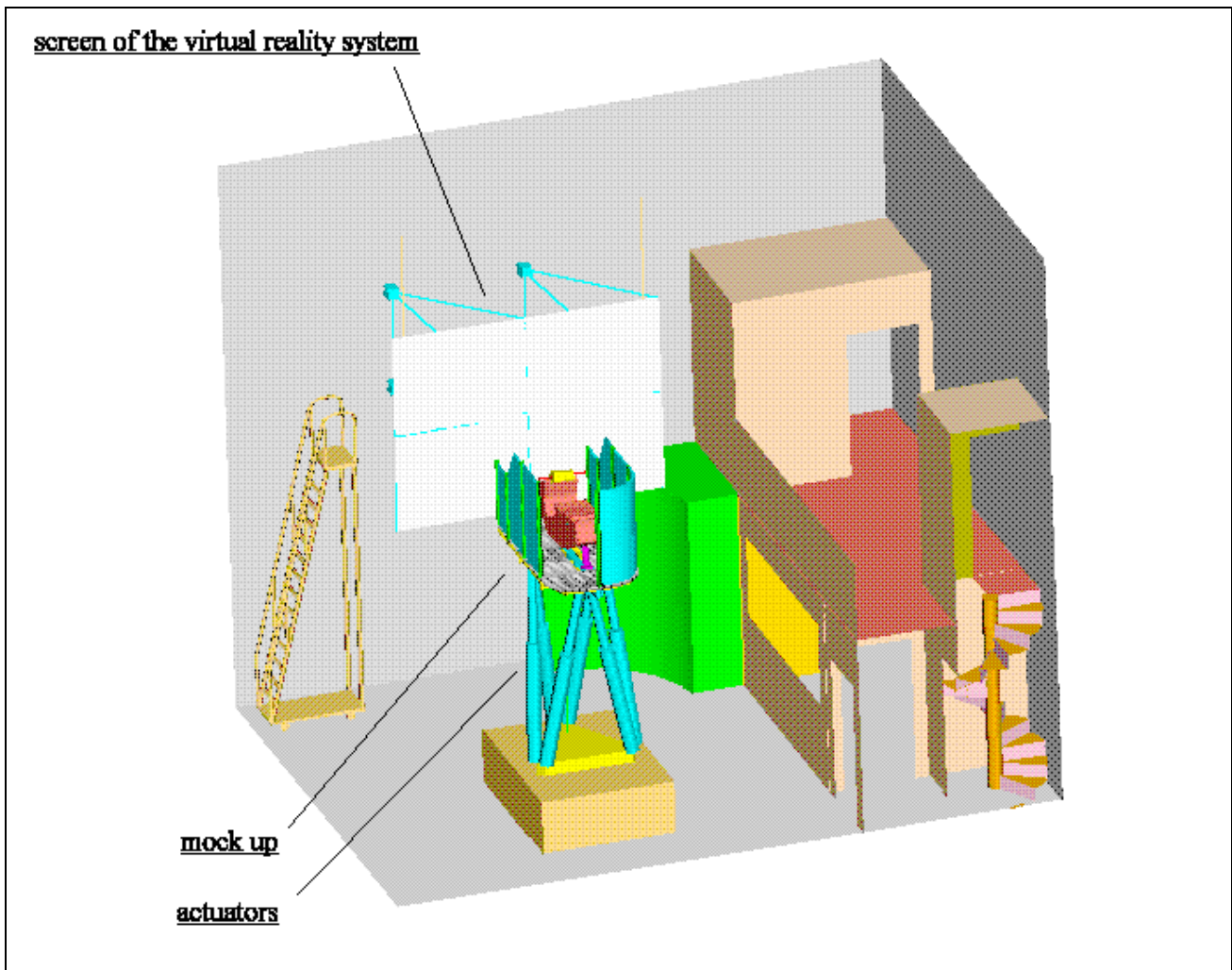
The object of the analysis was to evaluate relevant quantities to impart assigned acceleration time histories to a two-wheeled vehicle simulator, in the European MORIS project. Such quantities concern the actuator system of the simulator, which is constituted by a platform supported by six hydraulic pistons (Stewart platform).

## 2. THE PHYSICAL SYSTEM AND THE MULTIBODY MODEL

The physical system is made up of a mock-up of the vehicle which is fixed on a platform moved by 6 actuators, whose lower ends are connected to the ground. Each actuator is connected both to the ground and to the platform by a spherical joint. In this way the platform can move along each of its 6 degrees of freedom.

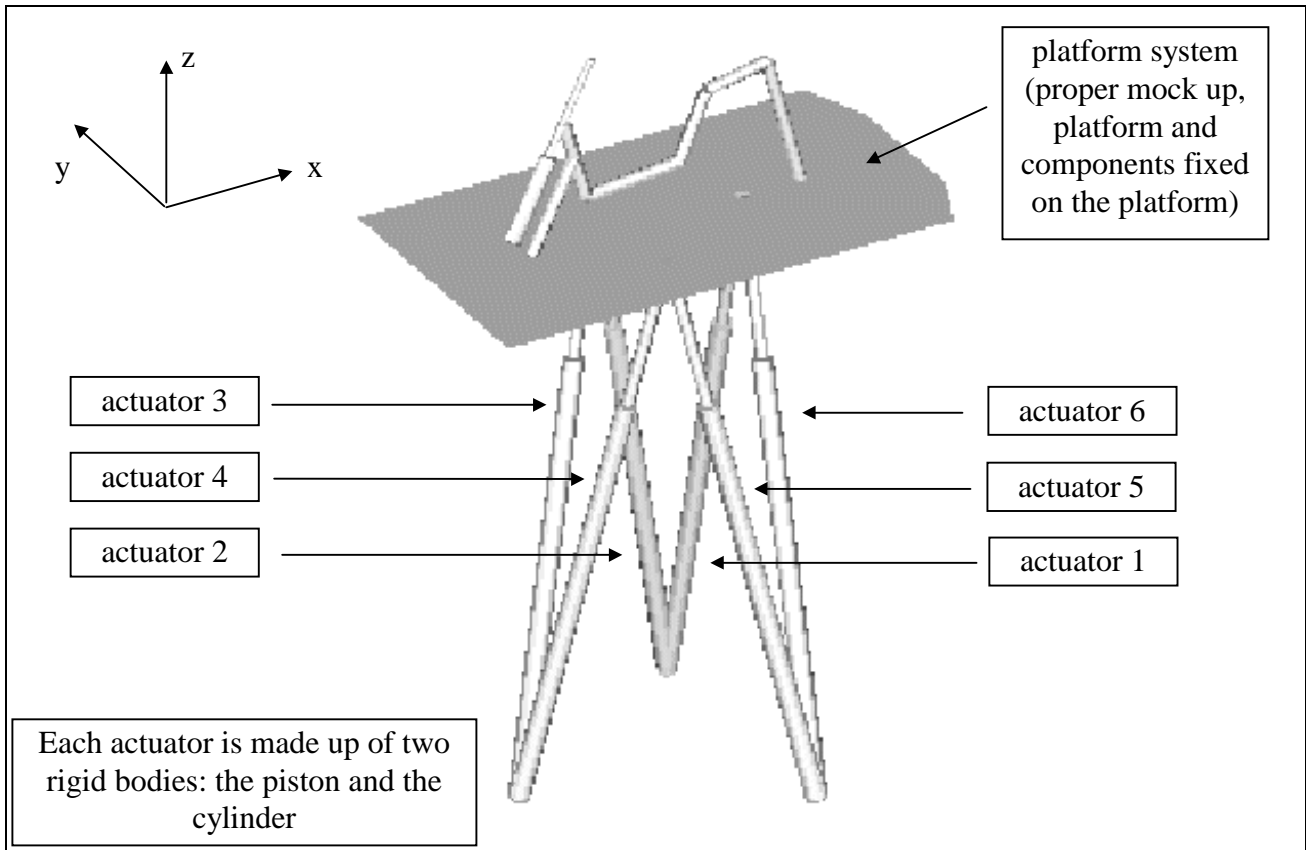
The other elements of the ride simulator, which are of no concern for the multibody analysis, are a virtual reality system with optical and acoustical elements, and the electronic control system.

The whole system is schematically shown in the following picture.



Picture 1. The physical system.

It was assumed that the mock-up and platform form an unique rigid body, together with other components fixed to the platform (e.g., a fan which simulates the wind). So the multibody model is made up of 13 rigid bodies, shown in the following pictures together with a conventional numbering of the actuators.



Picture 2. The multibody model.

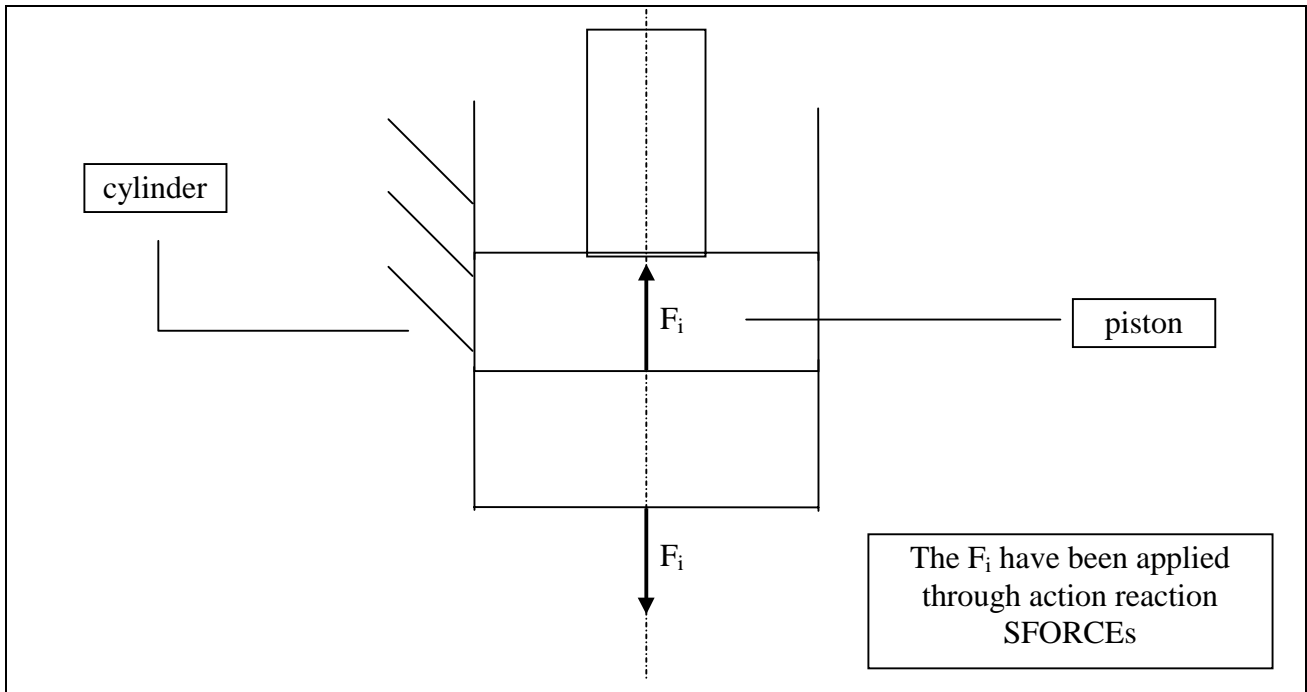
Since it was necessary to do a FEM analysis to make a first choice of the thickness of the platform, the inertial characteristics of the system (from now on called *platform system*) composed by the platform and the components mounted upon it, were computed by the FEM code.

The piston and the cylinder of each actuator have been connected by a translational joint, while spherical joints have been used to connect the platform to the pistons and the cylinders to the ground.

The joints between the platform and the pistons are located on a circle 400 mm in radius. The joints between the ground and the pistons are located on a circle 800 mm in radius. The height of the platform above the ground is 3360 mm.

### **3. THE LOADS**

In the model the external forces shown in the following picture were applied to each actuator:



Picture 3. The loads.

The  $F_i$  forces must impart a given acceleration time history to a point which moves rigidly with the platform system. The acceleration time history is experimentally determined during a typical manoeuvre.

In order to compute the  $F_i$  forces the following quantities have been defined:

$\mathbf{a}(t)$   $\equiv$  acceleration of the point the target acceleration is given at (both translational and rotational components)

$\mathbf{a}_o(t)$   $\equiv$  target acceleration (both translational and rotational components)

$\mathbf{F}(t)$   $\equiv$  vector whose components are the  $F_i$

$\mathbf{F}_0$   $\equiv$  vector whose components are the values of  $F_i$  at the static equilibrium of the system.

$\mathbf{A}; \mathbf{K}$   $\equiv$   $\mathcal{R}^{6 \times 6}$  matrixes

The vectors  $\mathbf{s}_o(t)$  e  $\mathbf{s}(t)$  have been defined too:

$$\mathbf{s}_o(t) = \mathbf{a}_o(t)$$

$$\mathbf{s}(t) = \mathbf{a}(t)$$

The following relation has been imposed:

$$\mathbf{F} = \mathbf{F}_0 + \mathbf{A}(\mathbf{a} - \mathbf{a}_o) + \mathbf{K}(\mathbf{s} - \mathbf{s}_o) \quad (1)$$

The following quantities have been defined

$$e_i \equiv \max_t |\mathbf{a}_{o_i} - \mathbf{a}_i|$$

The  $\mathbf{A}$  e  $\mathbf{K}$  matrixes have been defined with a trial and error procedure, in order to satisfy the following relations:

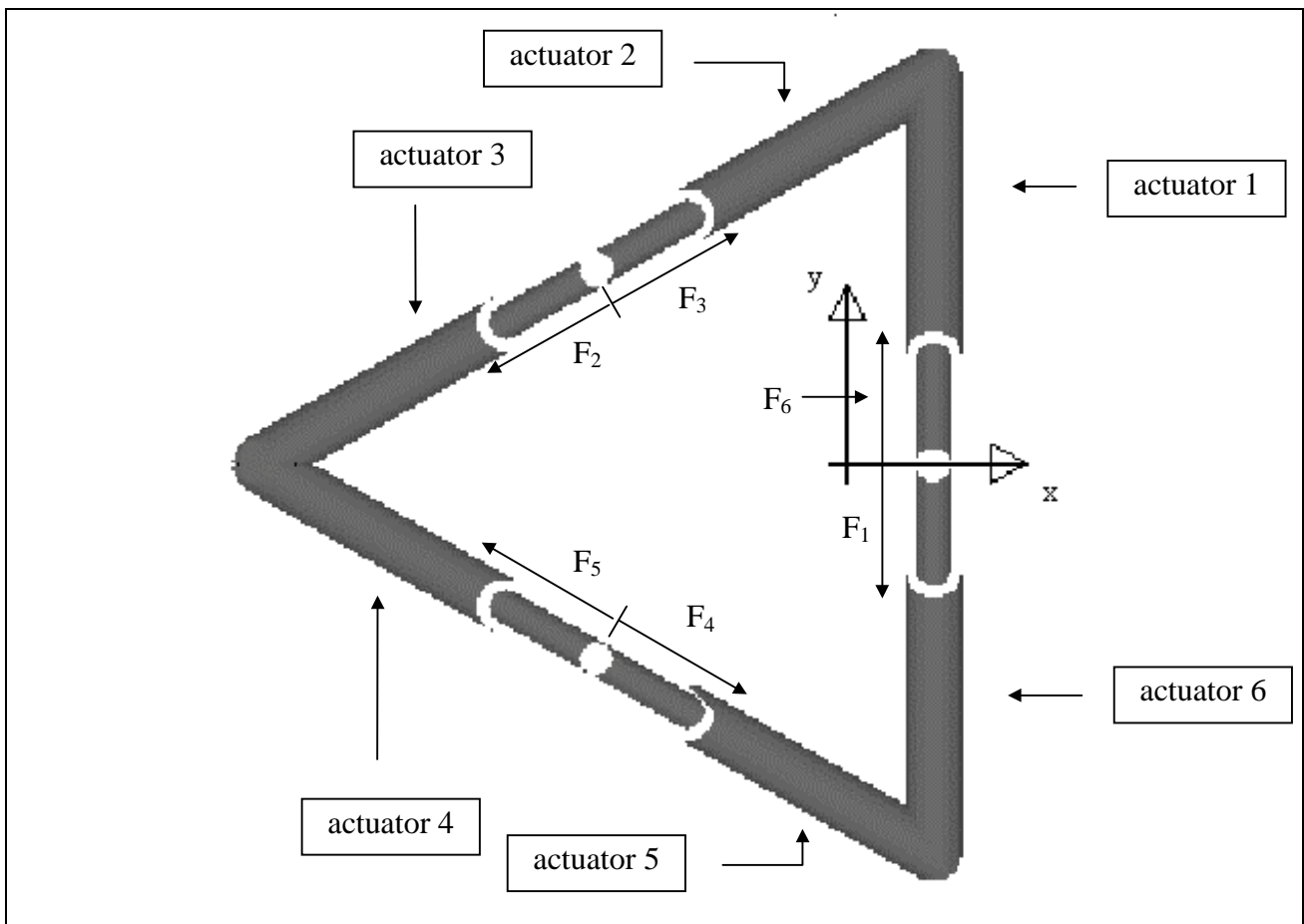
$$e_i < 10 \frac{\text{mm}}{\text{s}^2} \quad \text{if } i = 1,2,3$$

$$e_i < 0.5 \frac{\text{deg ree}}{\text{s}^2} \quad \text{if } i = 4,5,6$$

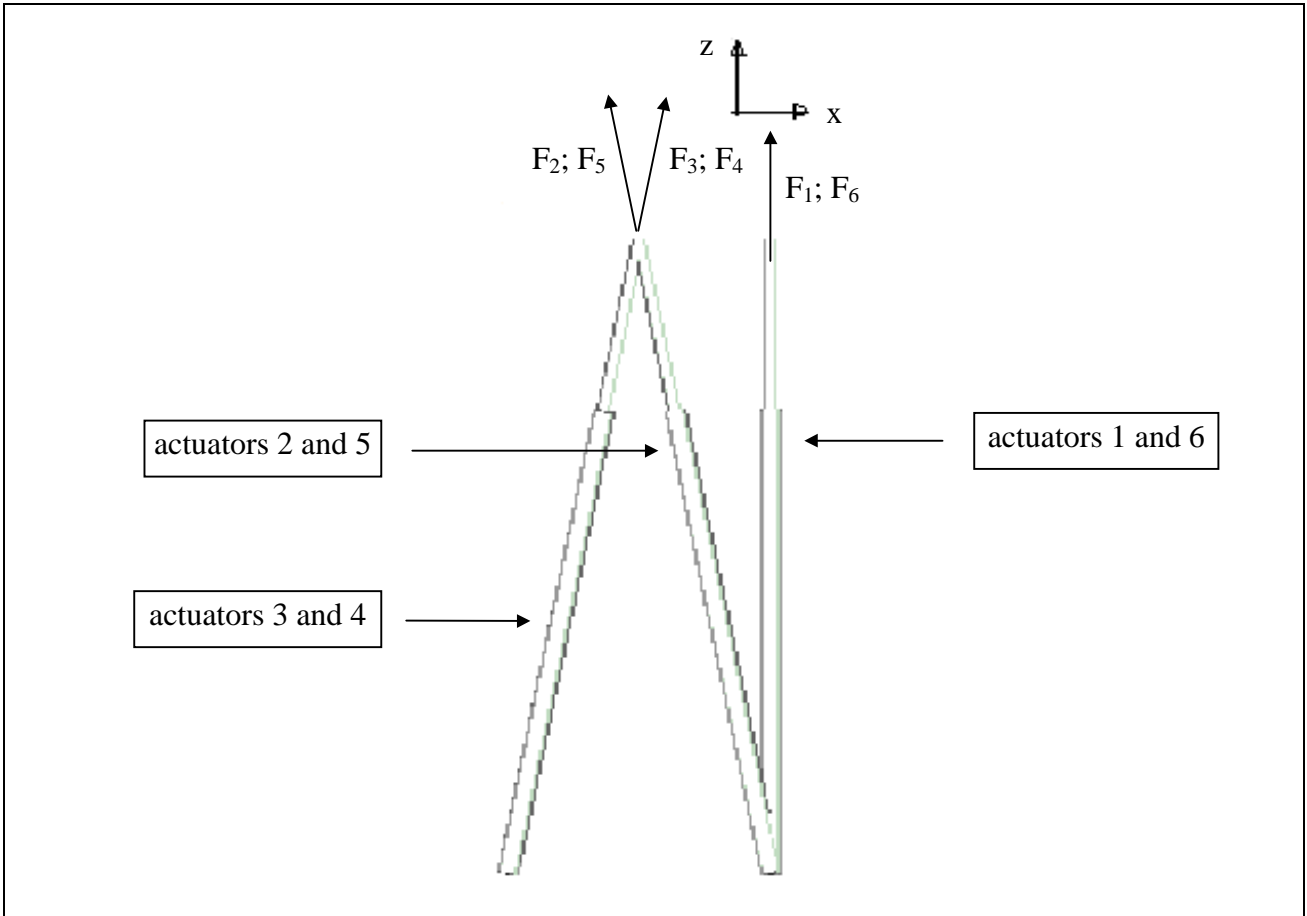
The maximum allowable values for  $e_i$  were chosen as one tenth of the acceleration accuracy of the class of actuators to be used.

The  $\mathbf{A}$  matrix represent an acceleration control. In particular, the  $i,j$  element of  $\mathbf{A}$  represent the control action exerted by the  $i$ -th actuator on the  $j$ -th component of acceleration. Similar remarks can be made about the  $\mathbf{K}$  matrix.

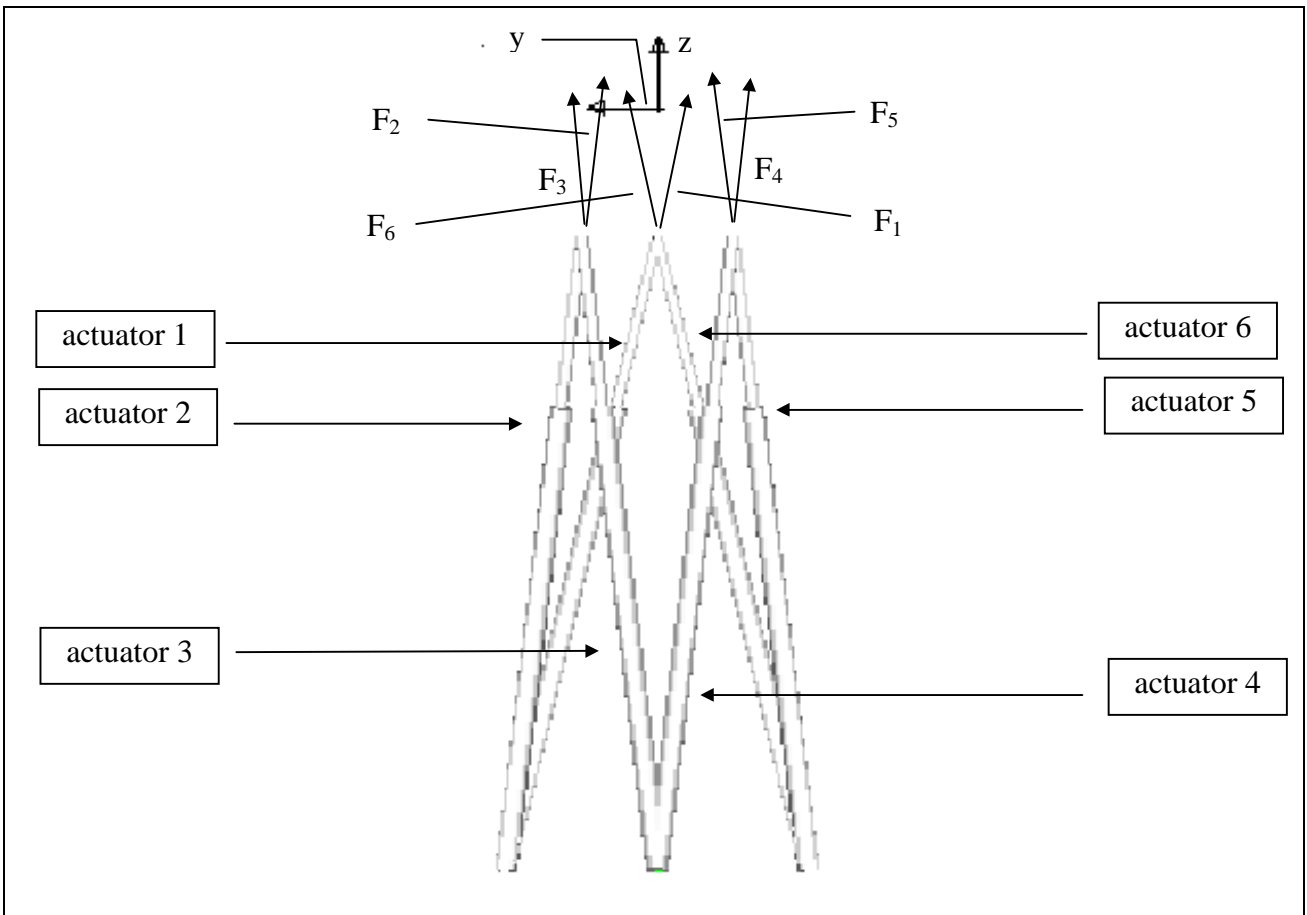
In the following pictures the three views of the actuators are shown, together with a triad with the origin in the point (called *reference point*) at which the target acceleration is given. In the pictures the directions along which the forces exerted by the actuators on the platform act are given.



Picture 4. xy view of the actuators.



Picture 5.  $xz$  view of the actuators.



Picture 6. yz view of the actuators.

Given the orientation of the actuators, only some elements of the **A** and **K** matrixes have been set non-zero. The structure of the **A** and **K** matrixes is shown in the following picture:

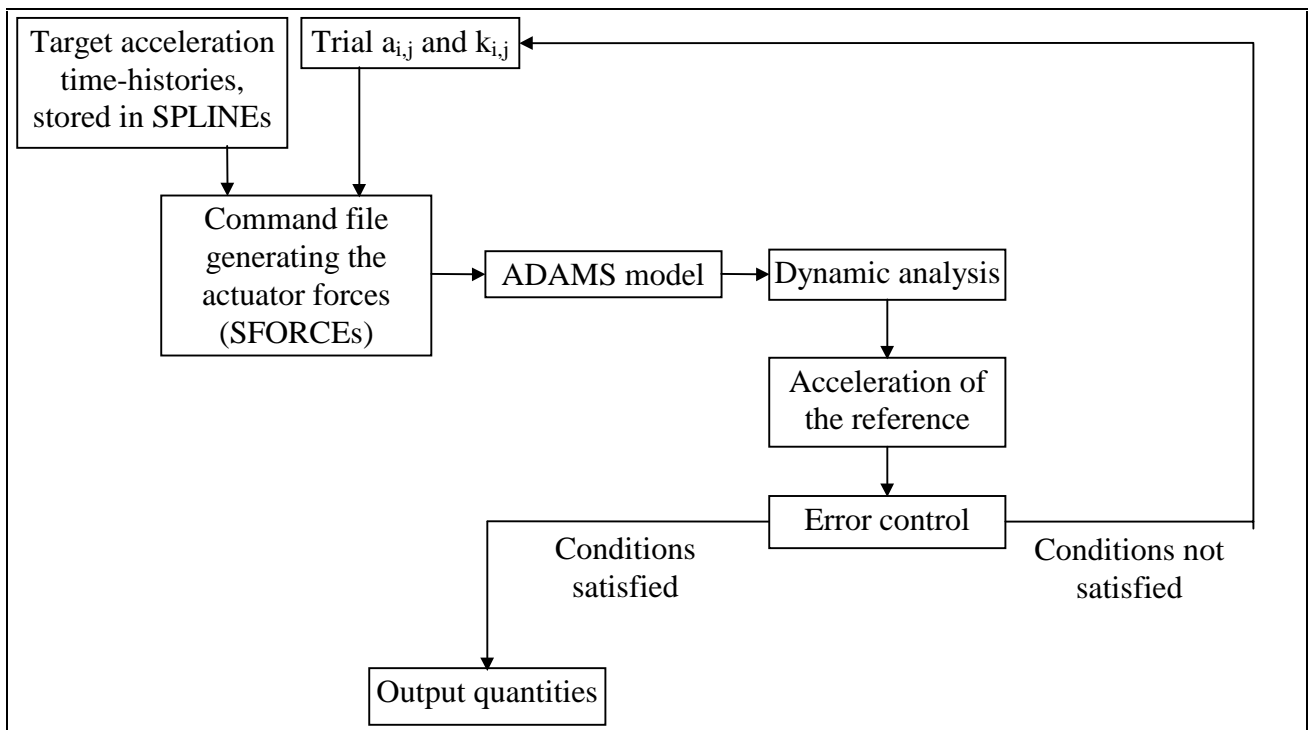
o	x	x	o	o	o
x	x	x	x	x	x
x	x	x	x	x	x
x	x	x	x	x	x
x	x	x	x	x	x
o	x	x	o	o	o

x = non-zero element  
o = zero element

Picture 7. Control matrixes structure.

#### **4. THE STRUCTURE OF THE MODEL**

The following flow chart describes how the model works.



Picture 8. Flow chart describing how the model works.

The output quantities are the following:



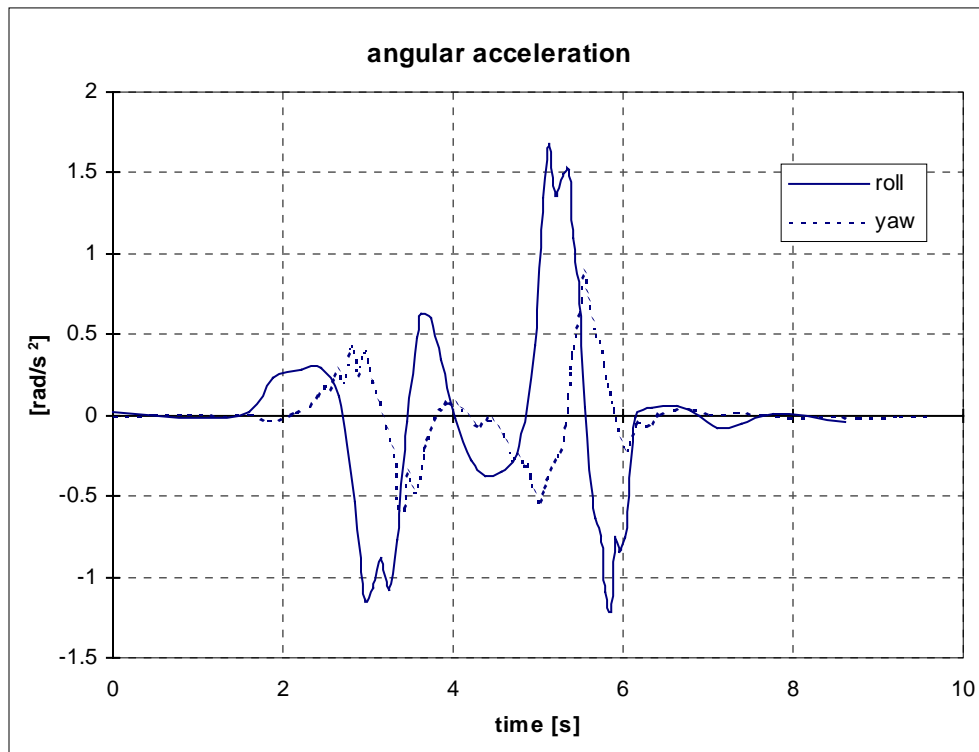
- the maximum power of each of the actuators;
- the maximum velocity of each piston relative to the respective cylinder;
- the maximum value of each displacement component of the reference point.

The first two outputs were used to give the requirements to the manufacturer of the actuators, while the last one was used to control whether the ride simulator comes out of the space it's supposed to stay in (the so called *working space*).

As an example, one of the analysed cases is reported in the following paragraph.

## **5. ONE OF THE ANALYSED CASES: LANE CHANGE MANOEUVRE**

The non zero components of the  $\mathbf{a}_0$  vector are the roll and the yaw ones. The experimental measures of the velocity components were the only ones available, so both numerical derivations and numerical integrations were needed in order to obtain the  $\mathbf{a}_0$  and the  $\mathbf{s}_0$  vectors. The non zero components of  $\mathbf{a}_0$  are shown in the following picture:



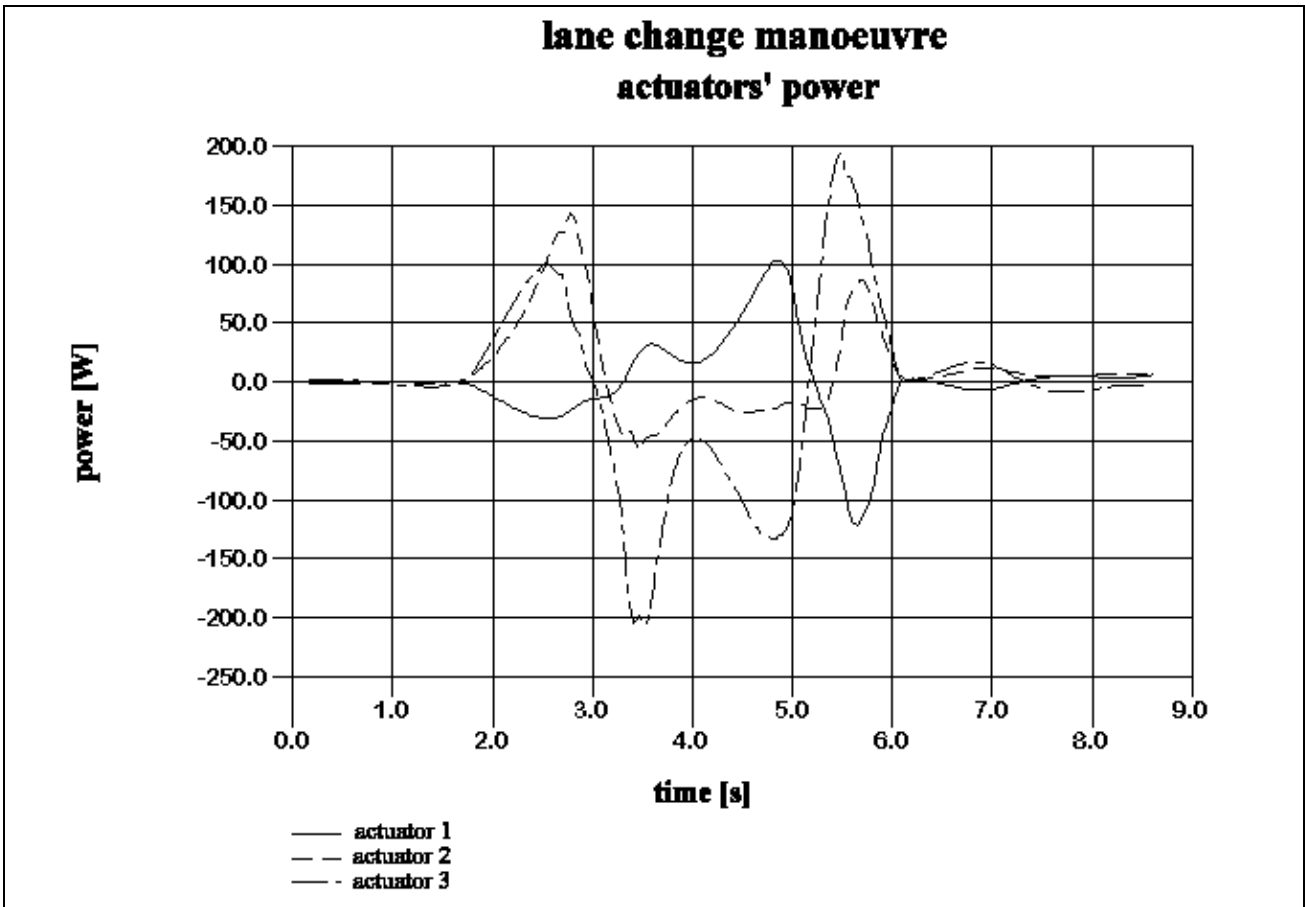
Picture 9. Lane change manoeuvre. Target acceleration components time histories.

The  $\mathbf{A}$  and  $\mathbf{K}$  matrixes turned out to be the following ones:

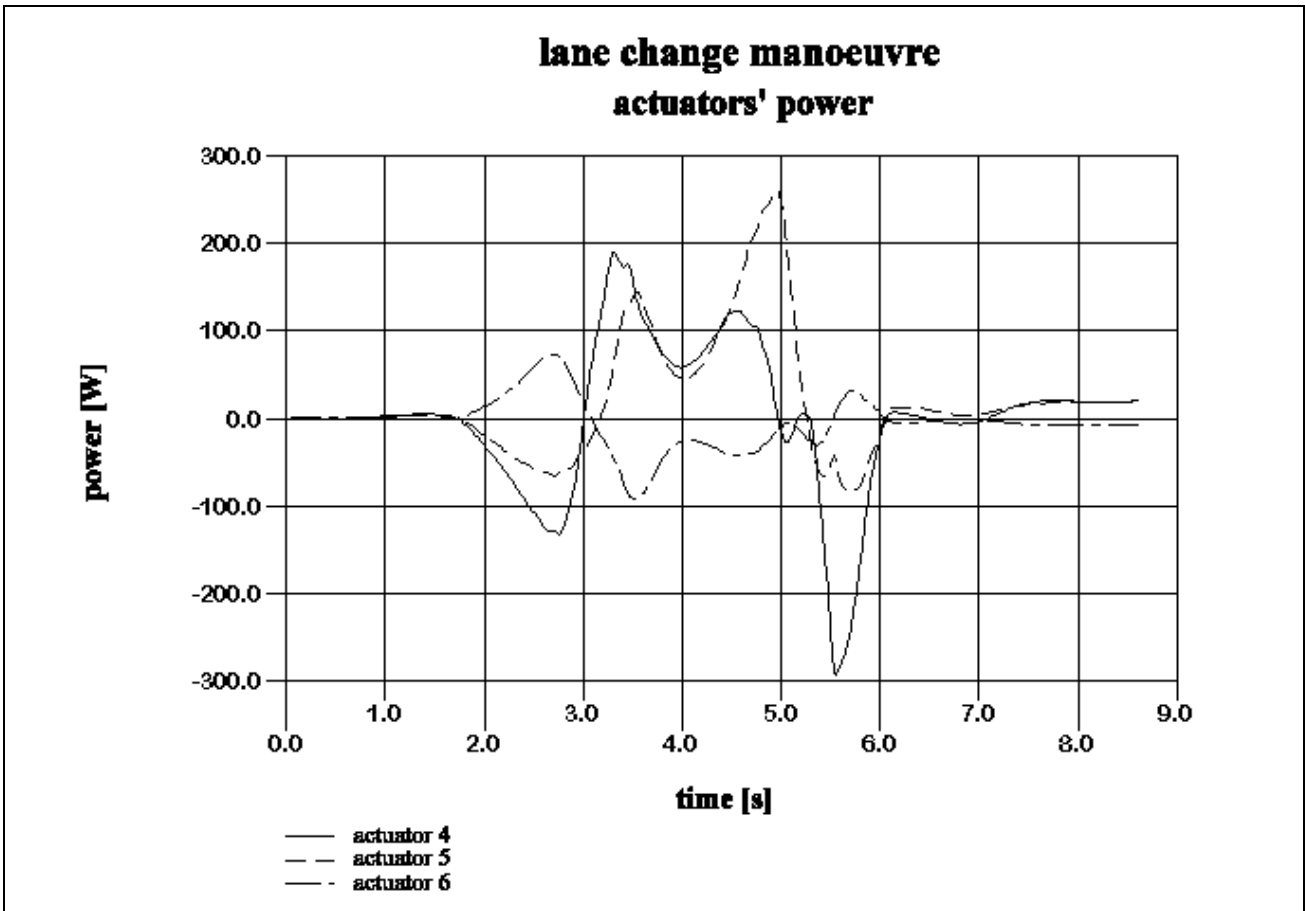
$$\mathbf{A} = \begin{pmatrix}
0 & 10^4 \frac{\text{N}}{\text{mm}} & -10^4 \frac{\text{N}}{\text{mm}} & 0 & 0 & 0 \\
100 \frac{\text{N}}{\text{mm}} & 10^4 \frac{\text{N}}{\text{mm}} & -10^4 \frac{\text{N}}{\text{mm}} & -5 \cdot 10^4 \frac{\text{N}}{\text{rad}} & -10^5 \frac{\text{N}}{\text{rad}} & -10^5 \frac{\text{N}}{\text{rad}} \\
-100 \frac{\text{N}}{\text{mm}} & -10^4 \frac{\text{N}}{\text{mm}} & -10^4 \frac{\text{N}}{\text{mm}} & -5 \cdot 10^4 \frac{\text{N}}{\text{rad}} & -10^5 \frac{\text{N}}{\text{rad}} & 10^5 \frac{\text{N}}{\text{rad}} \\
-100 \frac{\text{N}}{\text{mm}} & 10^4 \frac{\text{N}}{\text{mm}} & -10^4 \frac{\text{N}}{\text{mm}} & 5 \cdot 10^4 \frac{\text{N}}{\text{rad}} & -10^5 \frac{\text{N}}{\text{rad}} & -10^5 \frac{\text{N}}{\text{rad}} \\
100 \frac{\text{N}}{\text{mm}} & -10^4 \frac{\text{N}}{\text{mm}} & -10^4 \frac{\text{N}}{\text{mm}} & 5 \cdot 10^4 \frac{\text{N}}{\text{rad}} & -10^5 \frac{\text{N}}{\text{rad}} & 10^5 \frac{\text{N}}{\text{rad}} \\
0 & -10^4 \frac{\text{N}}{\text{mm}} & -10^4 \frac{\text{N}}{\text{mm}} & 0 & 0 & 0
\end{pmatrix}$$

$$\mathbf{K} = \begin{pmatrix}
0 & 0 & 0 & 0 & 0 & 0 \\
0 & 0 & 0 & 0 & 0 & 0 \\
0 & 0 & 0 & 0 & 0 & 0 \\
0 & 0 & 0 & 0 & 0 & 0 \\
0 & 0 & 0 & 0 & 0 & 0 \\
0 & 0 & 0 & 0 & 0 & 0
\end{pmatrix}$$

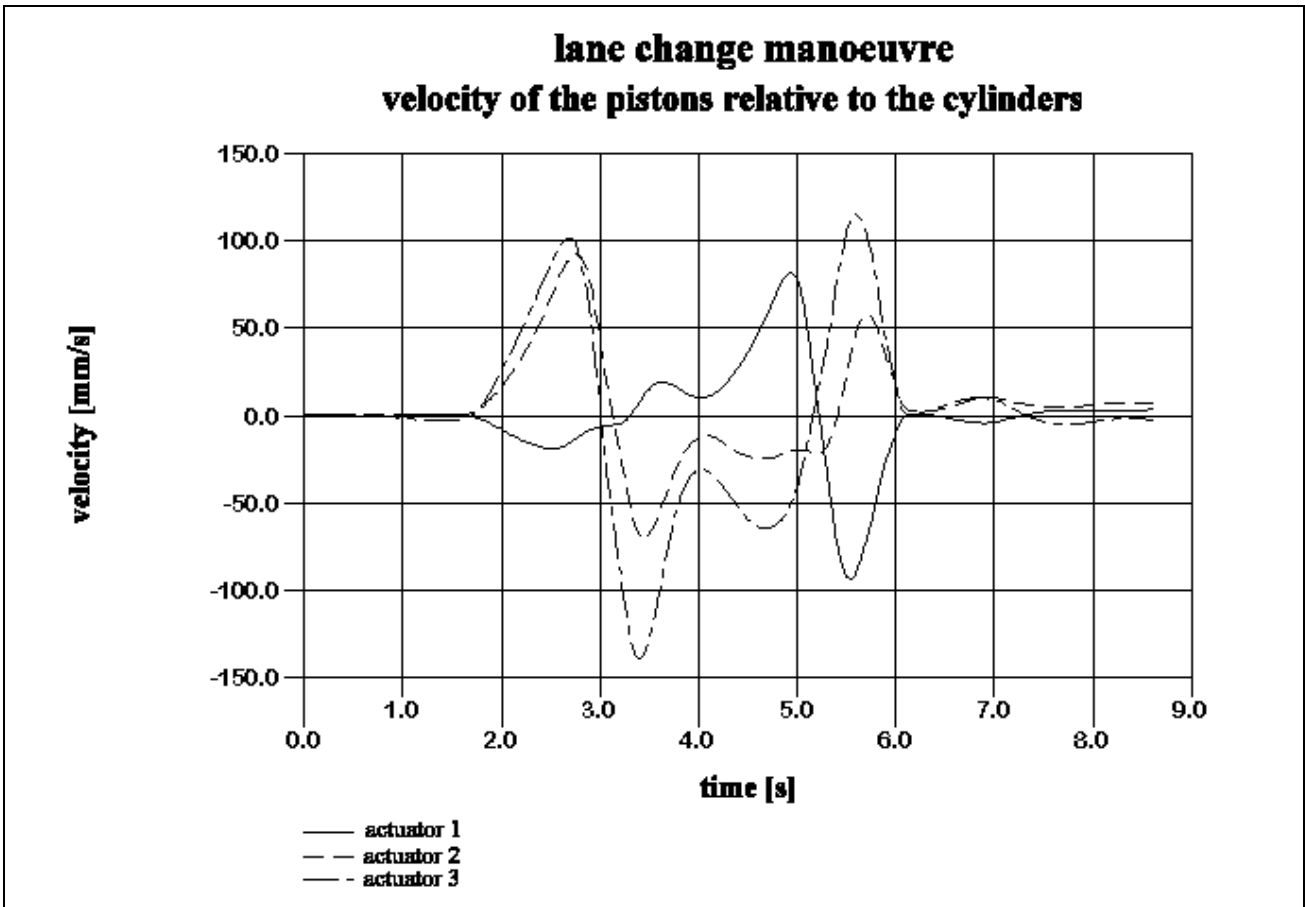
In other words, in this case only an acceleration control turned out to be necessary. In the following pictures are shown the outputs listed in paragraph 3.



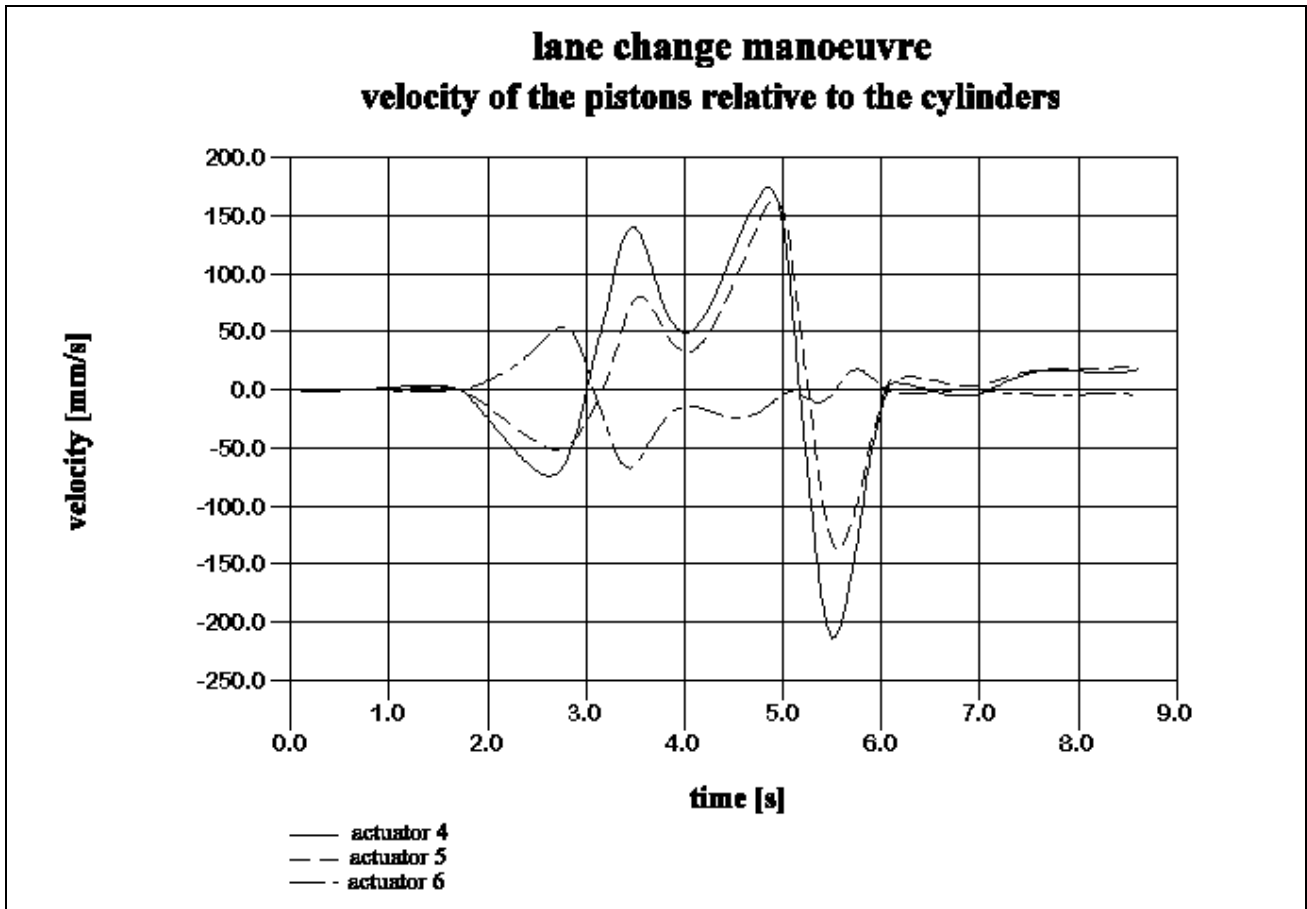
Picture 10. Lane change manoeuvre. Power of the actuators #1, 2 and 3.



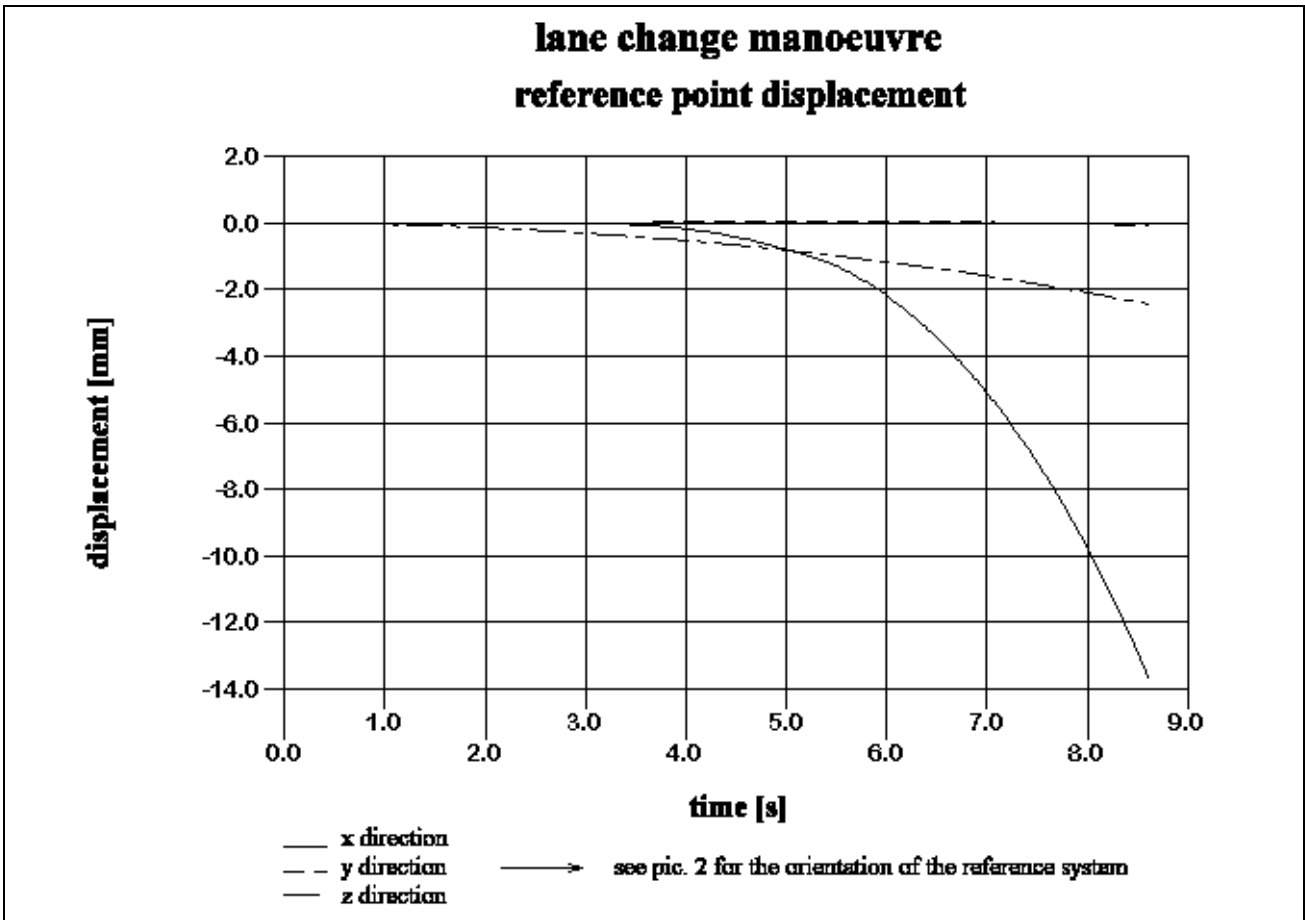
Picture 11. Lane change manoeuvre. Power of the actuators # 4, 5 and 6.



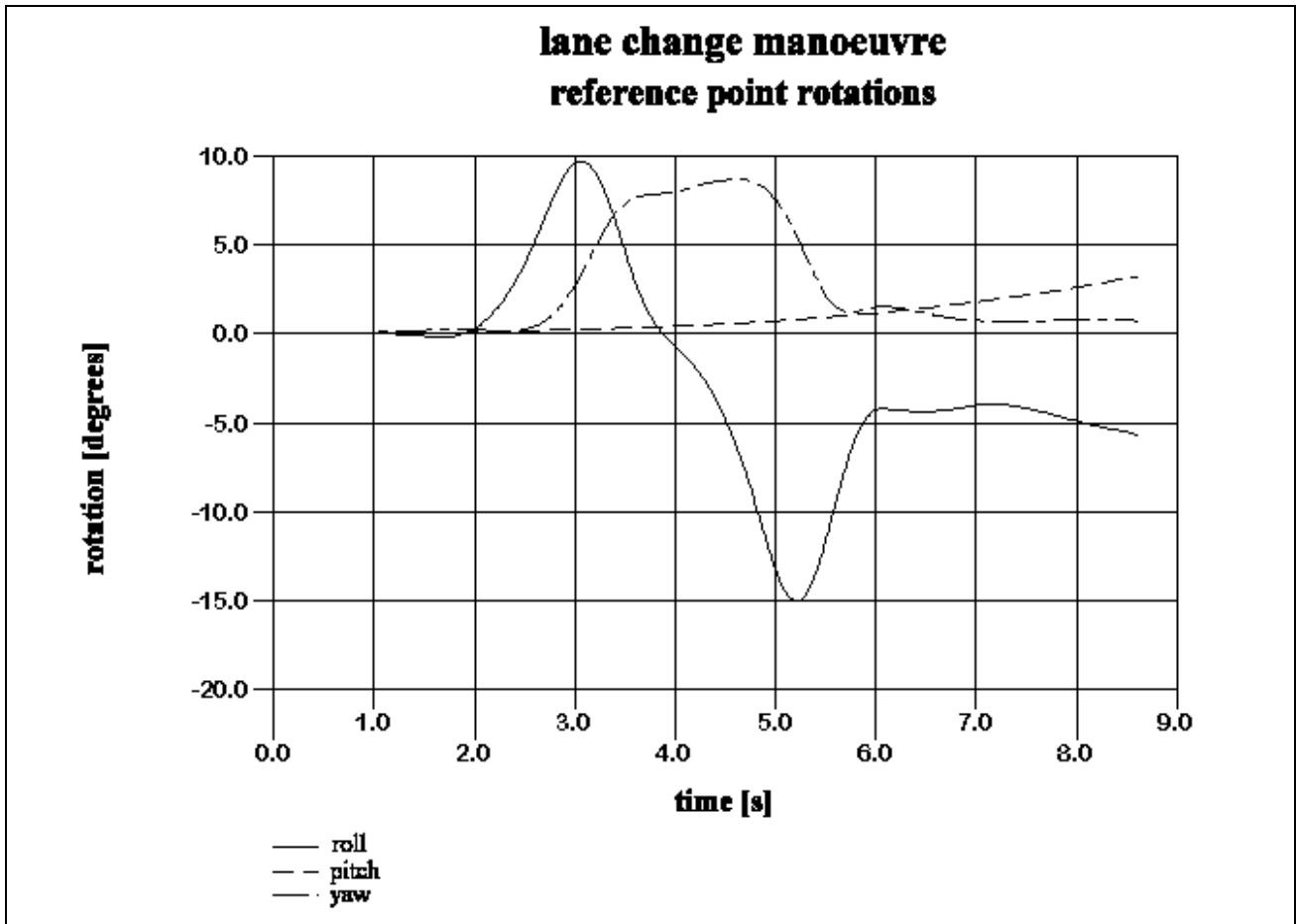
Picture 12. Lane change manoeuvre. Velocity of the pistons the actuators # 1, 2 and 3, relative to the cylinders.



Picture 13. Lane change manoeuvre. Velocity of the pistons the actuators # 4, 5 and 6, relative to the cylinders.



Picture 14. Lane change manoeuvre. Reference point displacement.



Picture 15. Lane change manoeuvre. Reference point rotations.

## 6. CONCLUSIONS

By means of a multibody model generated with ADAMS it was possible to estimate the power needed to impart specified accelerations to the ride simulator to be developed within the MORIS European Project, and to compute the kinematic behaviour of the system.